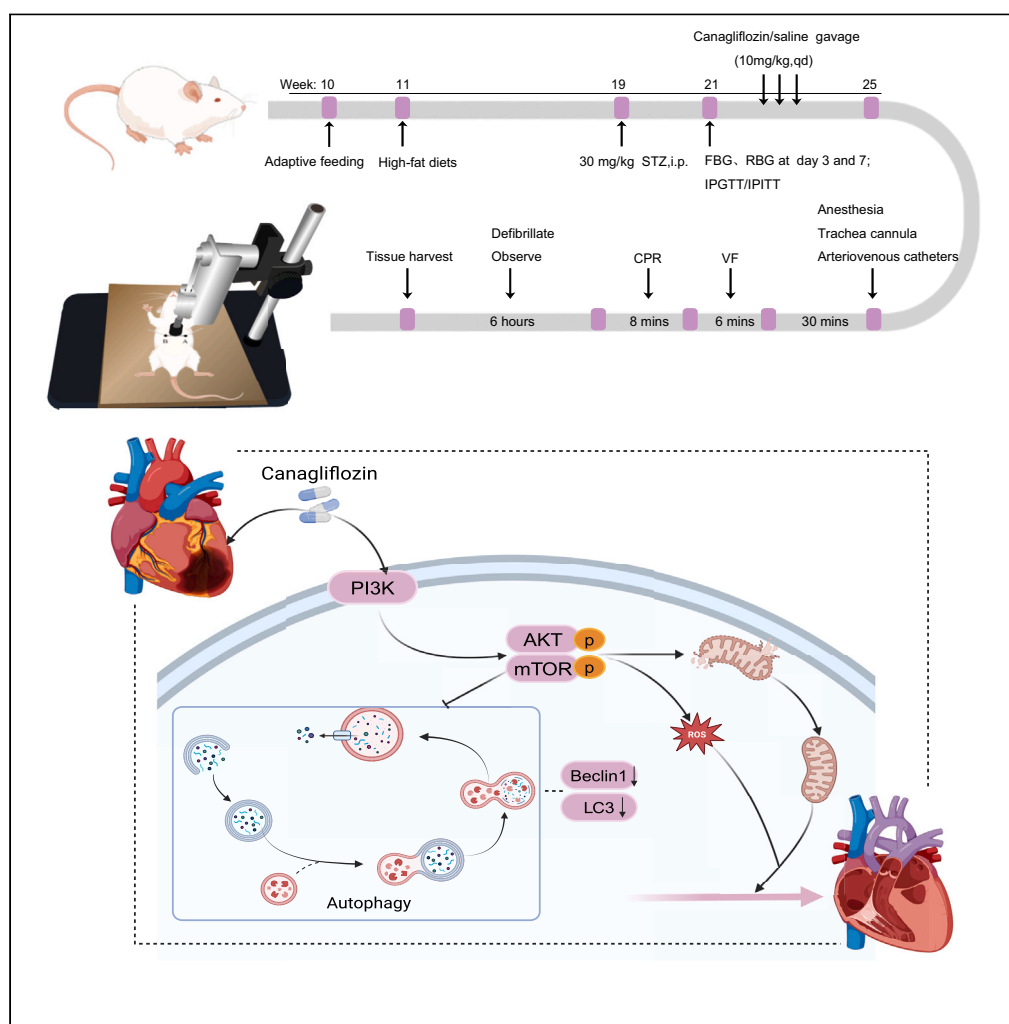


Article

Canagliflozin attenuates post-resuscitation myocardial dysfunction in diabetic rats by inhibiting autophagy through the PI3K/Akt/mTOR pathway



Qihui Huang, Wei Shi, Minjie Wang, ..., Wenyao Xiao, Tianfeng Hua, Min Yang

huatianfeng@ahmu.edu.cn (T.H.)
yangmin@ahmu.edu.cn (M.Y.)

Highlights

First study combining T2DM rats with modified epicardial VF model

Canagliflozin improves post-resuscitation myocardial dysfunction in T2DM rats

Canagliflozin activates PI3K/Akt/mTOR, reducing autophagy for cardioprotection

Huang et al., iScience 27, 110429
August 16, 2024 © 2024 The Author(s). Published by Elsevier Inc.
<https://doi.org/10.1016/j.isci.2024.110429>

Article

Canagliflozin attenuates post-resuscitation myocardial dysfunction in diabetic rats by inhibiting autophagy through the PI3K/Akt/mTOR pathway

Qihui Huang,^{1,2} Wei Shi,^{1,2} Minjie Wang,^{1,2} Liangliang Zhang,^{1,2} Yijun Zhang,^{1,2} Yan Hu,^{1,2} Sinong Pan,^{1,2} Bingrui Ling,^{1,2} Huaqing Zhu,³ Wenyan Xiao,^{1,2} Tianfeng Hua,^{1,2,4,*} and Min Yang^{1,2,4,5,*}

SUMMARY

This study investigated the effects of canagliflozin on myocardial dysfunction after cardiac arrest and cardiopulmonary resuscitation in diabetic rats and the underlying mechanisms. Male rats with type 2 diabetes mellitus (T2DM) were subjected to a modified epicardial fibrillation model. Pretreatment with canagliflozin (10 mg/kg/day) for four weeks improved ATP levels, post-resuscitation ejection fraction, acidosis, and hemodynamics. Canagliflozin also reduced myocardial edema, mitochondrial damage and, post-resuscitation autophagy levels. *In vitro* analyses showed that canagliflozin significantly reduced reactive oxygen species and preserved mitochondrial membrane potential. Using the PI3K/Akt pathway inhibitor Ly294002, canagliflozin was shown to attenuate hyperautophagy and cardiac injury induced by high glucose and hypoxia-reoxygenation through activation of the PI3K/Akt/mTOR pathway. This study highlights the therapeutic potential of canagliflozin in post-resuscitation myocardial dysfunction in diabetes, providing new insights for clinical treatment and experimental research.

INTRODUCTION

Diabetes mellitus is a major global public health challenge, with steadily increasing incidence and mortality rates.¹ Studies have shown that patients with diabetes have a 10-fold increased risk of sudden cardiac death compared with non-diabetic individuals. However, diabetic patients have significantly lower rates of return of spontaneous circulation (ROSC) and 30-day survival.^{2,3} The mortality rate for diabetic patients experiencing out-of-hospital cardiac arrest (OHCA) can be as high as 93.19%.⁴ Despite these significant implications, there are currently very few pharmacological treatments available in clinical practice for diabetes-related post-resuscitation myocardial dysfunction (PRMD).

Sodium-glucose cotransporter-2 inhibitors (SGLT-2i) are a class of well-known antidiabetic drugs that have attracted attention for their unique cardioprotective properties, which are independent of glycemic control. Prospective clinical trials, such as CANVAS and EMPA-REG OUTCOME, as well as comprehensive systematic meta-analyses, have consistently confirmed the potential of SGLT-2i to improve adverse cardiac events.^{5–7} Recent animal studies have provided new insights into the potential benefits of canagliflozin preconditioning for post-resuscitation myocardial protection.⁸ However, gaps in the knowledge of CA resuscitation in type 2 diabetic (T2DM) rats and the precise mechanisms are not yet fully elucidated.

A key mechanism by which diabetes exacerbates myocardial ischemia/reperfusion injury (I/RI) is the dysregulation of autophagy in diabetic myocardium. The PI3K/Akt/mTOR pathway is the only inhibitory pathway in the regulation of autophagy, capable of suppressing the expression of autophagy-related proteins such as Beclin-1 and LC3, thereby negatively modulating the autophagic process. In a hyperglycemic state, excessive reactive oxygen species (ROS) can reduce the binding efficiency of insulin receptor substrate-1 to PI3K/Akt, thereby disrupting the myocardial self-protection mechanism during diabetic I/RI.^{9,10} Therefore, modulation of the PI3K/Akt/mTOR pathway to restore autophagic function may represent a potential therapeutic strategy to ameliorate diabetic myocardial I/RI injury.

In view of those considerations, our study was designed to evaluate the effects of canagliflozin on PRMD in T2DM rats and to elucidate the underlying mechanisms, hoping to provide new insights for clinical treatment and experimental research.

¹The Second Department of Intensive Care Unit, The Second Affiliated Hospital of Anhui Medical University, Hefei 230601, Anhui, People's Republic of China

²The Laboratory of Cardiopulmonary Resuscitation and Critical Care Medicine, the Second Affiliated Hospital of Anhui Medical University, Hefei 230601, Anhui, People's Republic of China

³Laboratory of Molecular, Biology and Department of Biochemistry, Anhui Medical University, Hefei 230022, Anhui, People's Republic of China

⁴These authors contributed equally

⁵Lead contact

*Correspondence: huatianfeng@ahmu.edu.cn (T.H.), yangmin@ahmu.edu.cn (M.Y.)

<https://doi.org/10.1016/j.isci.2024.110429>



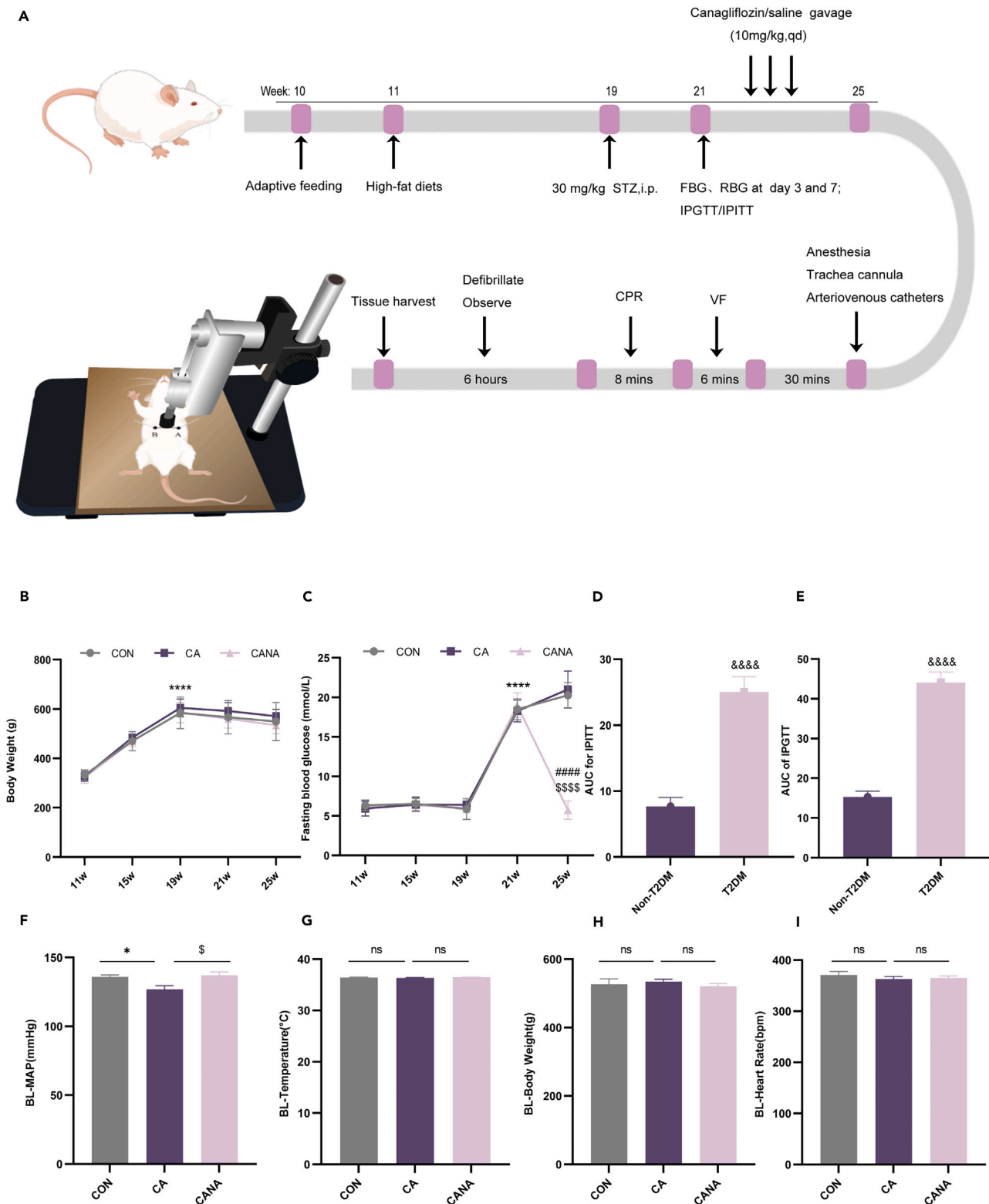


Figure 1. Flow of the model and baseline characteristics

(A) Flowchart of the type 2 diabetes mellitus (T2DM) and cardiac arrest/cardiopulmonary resuscitation (CA/CPR) modeling process in rats.

(B) Body weight changes in rats from 11 to 25 weeks.

Figure 1. Continued

(C) Fasting blood glucose (FBG) variations in rats from 11 to 25 weeks.

(D) AUC of the intraperitoneal glucose tolerance test (IPITT) in non-T2DM and T2DM rats.

(E) AUC of the intraperitoneal glucose tolerance test (IPGTT) in non-T2DM and T2DM rats.

(F) Comparison of baseline levels of mean arterial pressure (MAP) before CA/CPR operation between groups ($n = 6$).

(G) Comparison of baseline levels of temperature before CA/CPR operation between groups ($n = 6$).

(H) Comparison of baseline levels of body weight before CA/CPR operation between groups ($n = 6$).

(I) Comparison of baseline levels of heart rate before CA/CPR operation between groups ($n = 6$). Measurement data were presented as mean \pm SD. Differences among groups were determined by one-way ANOVA and LSD-test or Student's *t* tests. **** $p < 0.0001$, Comparison of FBG levels at 19 weeks vs. 21 weeks; ##### $p < 0.0001$, CANA versus CON group in 25 weeks; \$\$\$\$ $p < 0.0001$, CANA versus CA group in 25 weeks; &&&& $p < 0.0001$, non-T2DM versus T2DM rats; * $p < 0.05$, CON versus CA group; [§] $p < 0.05$, CA versus CANA group.

RESULTS**Baseline characteristics**

A total of 21 rats were used in this study. One rat was excluded due to unsuccessful T2DM modeling and two rats in the CA group were excluded due to failure to achieve ROSC. This resulted in a total of 18 rats for analysis. One rat failed resuscitation due to the inability to effectively control mean arterial pressure, and subsequent autopsy revealed large abscesses in its lungs. In another rat, autopsy after failed resuscitation revealed an abnormal heart position with a right-sided heart. No deaths were observed in the CON group. All rats in the CANA group were successfully resuscitated. After an acclimatisation period of 7 days, the rats were subjected to an 8-week high-fat dietary (HFD) intervention followed by treatment with streptozotocin (STZ) and canagliflozin (Figure 1A). Following the HFD, the average body weight of the three groups of rats significantly increased by 80.79% (11 weeks vs. 19 weeks, $p < 0.0001$, Figure 1B). Injection of STZ resulted in a significant elevation in fasting blood glucose (FBG) levels, with the average FBG levels increasing by 206.59% two weeks before and after STZ injection (18 weeks vs. 21 weeks) (6.07 vs. 18.61). Blood glucose levels decreased significantly after canagliflozin gavage in rats. In the CANA group, the mean FBG levels decreased by 69.89% (19.00 vs. 5.72) before and after the intervention (21 weeks vs. 25 weeks). Additionally, the reduction in FBG levels in the CANA group was statistically significant compared to the other groups (20.62 vs. 5.72, $p < 0.0001$, Figure 1C). To further assess glucose and insulin tolerance, tests were conducted on non-diabetic rats, revealing that diabetic rats had significantly lower glucose and insulin sensitivity compared to normal rats ($p < 0.05$, Figures 1D and 1E). Before performing CA/cardiopulmonary resuscitation (CPR), the vital signs of the rats were monitored, and it was found that the MAP levels in the CANA group were higher than those in the other groups ($p < 0.05$), while no significant differences in body weight, heart rate, and body temperature were observed among the groups (Figures 1F through 1I).

Canagliflozin improves hemodynamics and left ventricular function after resuscitation in T2DM rats

Monitoring changes in blood pressure 6 h in rats after CA/CPR revealed that the CA group exhibited unstable and consistently low mean arterial pressure (MAP) after resuscitation. In contrast, the CANA group showed a lower MAP within the first half hour after ROSC, which gradually increased thereafter (Figure 2A). Statistical trends of arterial blood gases over 6 h of ROSC, lactate (Lac) and base excess (BE) values showed significantly higher metabolic acidosis in the CA group. In contrast, canagliflozin significantly improved acidosis outcomes, indicating accelerated metabolic recovery post-resuscitation ($p < 0.05$, Figures 2B and 2C). Additionally, left ventricle ATP levels significantly decreased in diabetic rats post-resuscitation; however, canagliflozin increased energy reserves, with left ventricle ATP concentrations being higher than those in the CA group ($p < 0.05$, Figure 2H). During resuscitation, the cardiac function of rats was monitored, revealing that the left ventricular ejection fraction (LVEF) and left ventricular fractional shortening (LVFS) were lowest at 2 h post-resuscitation, and gradually improved around 4 h. The ejection capacity of the CA group was significantly lower than that of the CANA group at 2 h after resuscitation ($p < 0.05$, Figures 2F and 2G). Concurrent measurements of the left ventricular end-systolic volume (LVESV) and the left ventricular end-systolic dimension (LVD_s) revealed significant increases in both parameters in the post-resuscitation rats. These increases indicate a decline in left ventricular contractile function and pronounced ventricular dilation, suggesting potential left ventricular dysfunction. However, pretreatment with canagliflozin significantly reduced LVESV and LVD_s after resuscitation, effectively alleviating cardiac injury in diabetic rats ($p < 0.05$, Figures 2I and 2J). Compared to the CA group, the CANA group demonstrated significantly better left ventricular function at 2, 4, and 6 h post-resuscitation and canagliflozin reduced the frequency of post-resuscitation arrhythmias in rats (Figures 2D and 2H).

Canagliflozin attenuates myocardial injury after resuscitation in T2DM rats by downregulating autophagy protein

To assess the potential ameliorative induction of canagliflozin on pathological changes in myocardial I/RI of T2DM rats, we evaluated post-resuscitation myocardial tissue damage using transmission electron microscopy (TEM) and hematoxylin-eosin (HE) staining. TEM revealed significant ultrastructural changes in the myocardial tissue of CA group in comparison to CON group, including sarcomere disruption, mitochondrial swelling and deformation, partial outer mitochondrial membrane rupture, cristae disappearance, and the presence of numerous autophagosomes and autolysosomes. In contrast, rats treated with canagliflozin exhibited marked improvements in mitochondrial morphology, with a reduction in the number of autophagosomes (Figure 3G). After HE staining of myocardial tissue, the CA group exhibited significant myocardial tissue edema, myocardial cell and interstitial blur, and rupture, as well as disordered arrangement of myocardial fibers

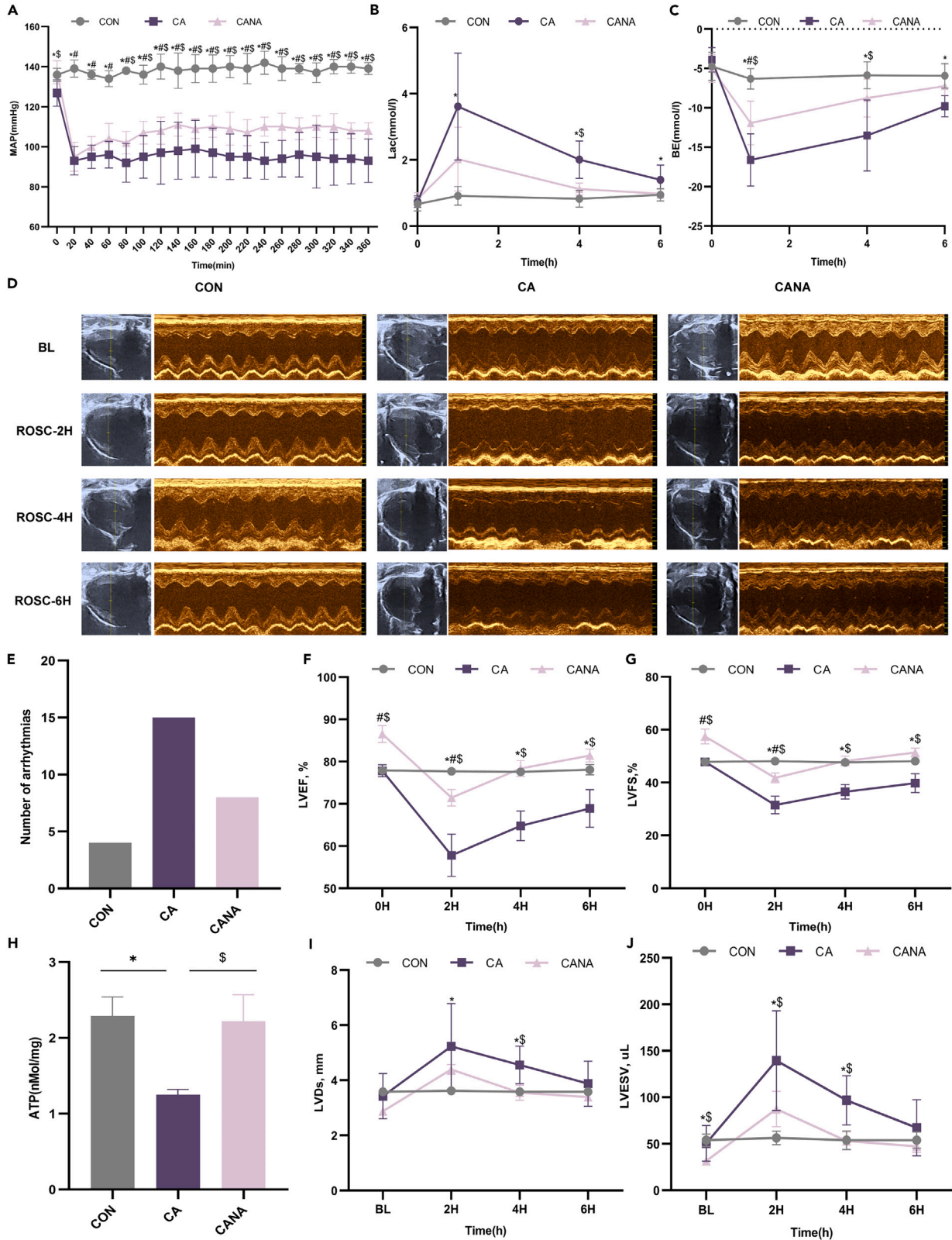


Figure 2. Effects of canagliflozin on hemodynamics and left ventricular function in T2DM rats after resuscitation

- (A) Trends in mean arterial pressure (MAP) within 6 h after-restore of spontaneous circulation (ROSC) ($n = 6$).
(B) Comparative levels of lactate (Lac) in arterial blood between groups ($n = 6$).
(C) Comparative levels of base excess (BE) in arterial blood between groups ($n = 6$).
(D) Echocardiographic assessments at baseline (BL), 2, 4, and 6 h after-ROSC ($n = 6$).
(E) The number of arrhythmias after ROSC between groups ($n = 6$).
(F) Comparison of left ventricular ejection fractions (LVEF) between groups ($n = 6$).
(G) Comparison of left ventricular fractional shortening (LVFS) between groups ($n = 6$).
(H) Comparison of ATP content in left ventricular tissue between groups ($n = 6$).
(I) Comparison of left ventricular end-systolic volume (LVESV) between groups ($n = 6$).
(J) Comparison of left ventricular end-systolic dimension (LVD_s) between groups ($n = 6$). Measurement data were presented as mean \pm SD. Differences among groups were determined by one-way ANOVA and LSD-test. * $p < 0.05$, CON versus CA group; # $p < 0.05$, CON versus CANA group; \$ $p < 0.05$, CA versus CANA group.

when compared to the CON group. In comparison to the CA group, the CANA group observed a marked reduction in edema and damage, with a more orderly arrangement of myocardial fibers (Figure 3A).

Our analysis concurrently revealed that, relative to the CON group, myocardial injury markers creatine kinase-MB (CK-MB) and lactate dehydrogenase (LDH) showed a marked elevation in the CA group. In contrast, the CANA group showed a lesser extent of myocardial damage ($p < 0.05$, Figures 3C and 3D). To further determine whether the benefits on myocardial tissue of canagliflozin are related to autophagy, the expression of autophagy in myocardial tissue was detected. An evident upsurge in the autophagic proteins LC3II/I and Beclin 1 was observed in the CA group in comparison to the CON group. However, canagliflozin treatment appeared to suppress the overexpression of these autophagic proteins ($p < 0.05$, Figures 3B, 3E, and 3F). These findings imply that canagliflozin administration may diminish autophagic levels in myocardial tissue and notably ameliorate myocardial I/R in T2DM rats following resuscitation.

Canagliflozin improves H/R injury of H9c2 cardiomyocytes in high glucose environment

We investigated the potential protective effect of canagliflozin pretreatment on hypoxic reoxygenation of H9c2 cells by utilizing a high glucose hypoxia reoxygenation (HG + H/R) model on H9c2 cardiomyocytes. Cell Counting Kit-8 experiments demonstrated that the addition of canagliflozin significantly improved the viability of cells subjected to H/R compared to the HG + H/R group ($p < 0.05$, Figure 4A). We further evaluated oxidative stress and mitochondrial dysfunction by assessing changes in ROS levels and mitochondrial membrane potential (MMP). The model group exhibited significantly higher levels of ROS and MMP, whereas canagliflozin mitigated the severity of oxidative stress and significantly reduced mitochondrial damage (Figures 4H and 4I). These findings were consistent with a marked decrease in LDH activity and the oxidative index malondialdehyde (MDA) ($p < 0.05$, Figures 4B and 4C). The results indicate that canagliflozin effectively ameliorates oxidative stress and mitochondrial damage induced by HG + H/R. To further evaluate this, we assessed the changes in cellular ATP levels following reoxygenation. Under HG + H/R injury, ATP levels were significantly reduced. However, treatment with canagliflozin increased ATP production, thereby improving cellular energy status ($p < 0.05$, Figure 4D). The impact of canagliflozin on autophagy in cardiomyocytes under HG + H/R injury was also investigated. LC3II/I and Beclin 1 protein expression levels were notably increased in H9c2 cardiomyocytes of the HG + H/R group when compared to the CON group. However, canagliflozin effectively reversed the extent of increased autophagy, yielding statistically significant differences ($p < 0.05$, Figures 4E through 4G). In summary, our results demonstrate that canagliflozin pretreatment improves cell viability, reduces intracellular oxidative stress, ameliorates mitochondrial dysfunction, decreases LDH activity, and attenuates persistent autophagy in cardiomyocytes induced by HG + H/R injury conditions.

Canagliflozin inhibits autophagy through the PI3K/Akt/mTOR pathway to exert myocardial protection

To explore the relationship between autophagy regulation and the PI3K/Akt/mTOR pathway, we employed a co-incubation approach using the PI3K inhibitor Ly294002 in conjunction with canagliflozin to inhibit activation of the PI3K/Akt pathway in H9c2 cardiomyocytes. Our goal was to assess alterations in cardiomyocyte autophagy and determine whether the efficacy of canagliflozin would be reduced. We observed that canagliflozin significantly promoted cell viability after HG + H/R. Remarkably, the positive effects of canagliflozin on cell viability were negated when Ly294002 was added in the HG + H/R + CANA group ($p < 0.05$, Figure 5A). Furthermore, we examined mitochondrial function using fluorescence microscopy and found that the addition of Ly294002 counteracted the protective impact of canagliflozin on mitochondrial function. This was demonstrated by a substantial increase in JC-1 green fluorescent monomers and a decline in mitochondrial membrane potential (Figure 6D). Compared to the HG + H/R + CANA group, the HG + H/R+CANA+Ly294002 group exhibited significantly elevated levels of LDH activity, MDA, and ROS oxidation, further indicating the reversal of canagliflozin's myocardial protective effects (Figures 5B, 5C, and 5I). In addition, results showed that pretreatment with canagliflozin activated the phosphorylation of p-Akt/Akt protein expression levels, significantly increased the ratio of phosphorylated p-mTOR/mTOR, and reduced the protein levels of the autophagy markers LC3 II/I and Beclin 1. However, the addition of Ly294002 markedly reversed the expression levels of the pathway proteins, inhibited p-mTOR/mTOR protein expression, and attenuated canagliflozin inhibition of autophagy in myocardial cells ($p < 0.05$, Figures 5D through 5H). Furthermore, to elucidate the relationship between the canagliflozin and the PI3K/Akt/mTOR pathway, we conducted validation experiments on myocardial tissue from animals. The results demonstrated that pretreatment with canagliflozin activated

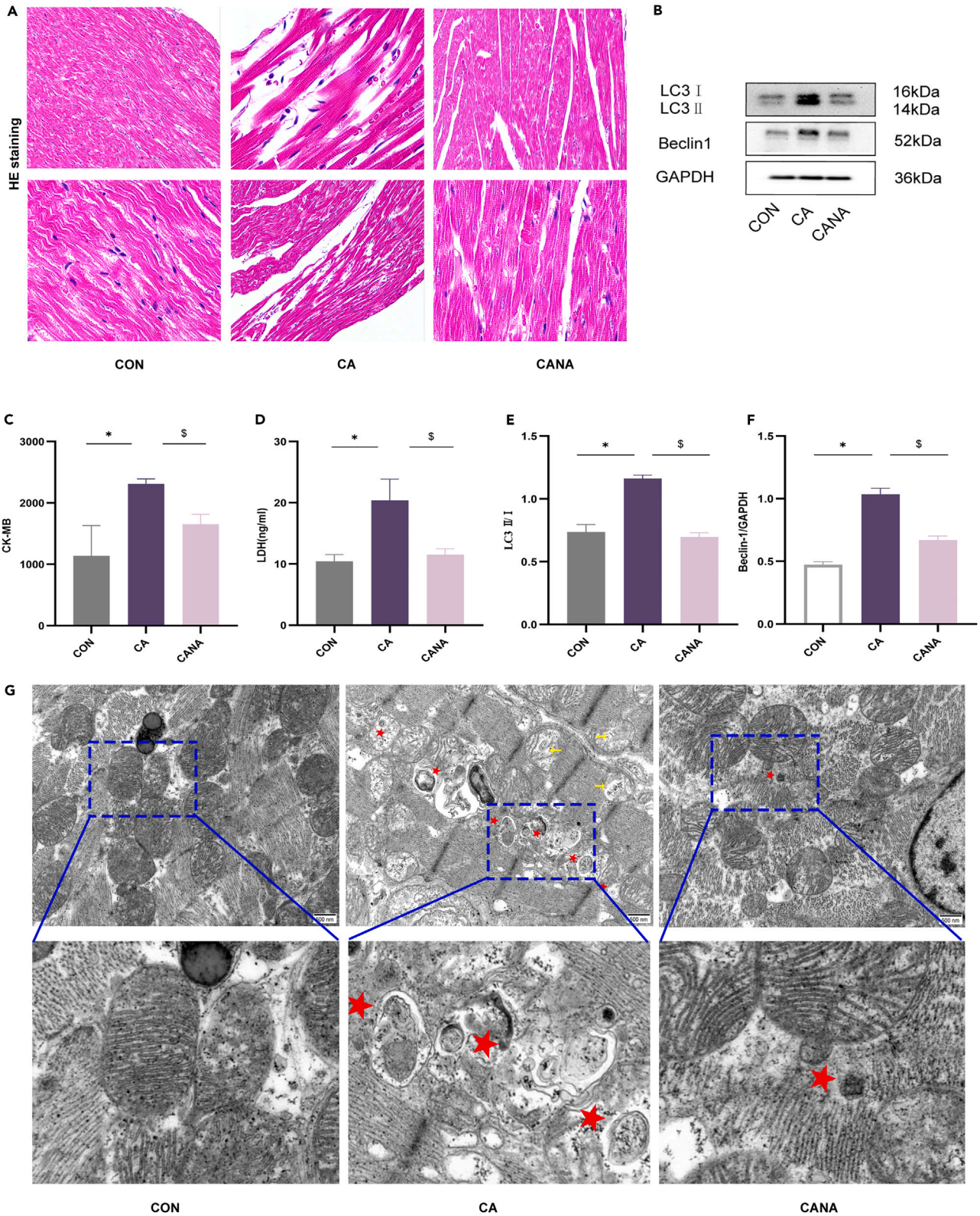


Figure 3. Canagliflozin attenuates myocardial structural damage by reducing autophagy levels

(A) Hematoxylin-eosin (HE) staining of myocardial tissue in ROSC rats using pathological sections, Magnification, $\times 100$ and $\times 400$.

(B) Representative protein bands of LC3II/I, Beclin 1, and GAPDH.

(C) Comparison of myocardial tissue creatine kinase isoenzyme MB (CK-MB) levels between groups ($n = 6$).

(D) Comparison of myocardial tissue lactate dehydrogenase (LDH) levels between groups ($n = 6$).

(E) Quantitative analysis of myocardial tissue LC3II/I protein expression levels ($n = 3$).

(F) Quantitative analysis of myocardial tissue Beclin 1 protein expression levels ($n = 3$).

(G) Ultra pathological changes in myocardial tissue by transmission electron microscopy in various groups of rats. Autophagosomes (red asterisks); damaged mitochondria (yellow arrows), Magnification, $\times 10000$ and $\times 25000$. Measurement data were presented as mean \pm SD. Differences among groups were determined by one-way ANOVA and LSD-test. $^*p < 0.05$, CON versus CA group; $^{\$}p < 0.05$, CA versus CANA group.

the expression levels of p-Akt/Akt and p-mTOR/mTOR proteins ($p < 0.05$, Figures 6A through 6C). Taken together, these data provide evidence that canagliflozin may protect cardiomyocytes against I/RI by modulating autophagy levels through the PI3K/Akt/mTOR pathway.

DISCUSSION

In the current study, we investigated the effects and mechanisms of canagliflozin on cardiac function after CA/CPR in T2DM rats. Our results demonstrated that canagliflozin pretreatment significantly alleviated PRMD, as evidenced by improved myocardial tissue structure, reduced levels of indicators of heart injury (CK-MB and LDH), a decrease in the incidence of arrhythmias, improved myocardial contractility and ATP content. Further investigation revealed that these benefits are linked to a reduction in autophagy. Through in vitro experiments, we discovered that canagliflozin pretreatment exerts its effects by activating the PI3K/Akt/mTOR pathway to reduce autophagy levels, which reduces oxidative stress and improves mitochondrial function after myocardial I/RI. It provides a valuable therapeutic approach for managing PRMD in diabetes patients.

PRMD is defined as reversible dysfunction caused by stunned myocardium without coronary artery occlusion.¹¹ Evidence suggests that more than 30% of all mortality in the first 72 h after CPR can be attributed to PRMD.¹² The pathophysiological mechanism of PRMD is myocardial I/RI. Previous studies have shown that diabetes not only increases susceptibility to myocardial I/RI but also that diabetes combined with myocardial I/RI increases infarct size by approximately 50% compared to non-diabetic patients, which may lead to more severe PRMD and poorer prognosis.^{13–15} The mechanisms responsible for this deterioration are not clearly understood, but oxidative stress, mitochondrial dysfunction, and dysregulation of autophagic balance associated with hyperglycemia may play crucial roles.¹⁶ Disturbances in lipid and glucose metabolism in diabetic myocardial cells trigger various damage mechanisms, including the formation of the polyol pathway and advanced glycation end products.¹⁷ This results in the overproduction of superoxide inside the mitochondrial electron transport chain, which inhibits glycolytic enzymes, causing alterations in cellular pathways and exacerbating oxidative stress.¹⁸ Mitochondrial dysfunction occurs earliest in diabetes mellitus combined with myocardial I/RI, as evidenced by mitochondrial swelling, cristae rupture, and cessation of oxidative phosphorylation, which causes lactate accumulation and calcium overload, leading to decreased myocardial contractility and cellular metabolic disturbances. In addition, hyperglycemia reduces the activity of antioxidant enzymes, which leads to an increase in ROS and mitochondrial dysfunction, creating a vicious circle.¹⁹ Our findings indicate that despite the recovery of myocardial automaticity within 30 min of ROSC, overall cardiac function remains severely impaired. Characteristic features include significant hemodynamic deterioration, intracellular acidosis, and myocardial pathological changes such as edema, myofiber rupture, and mitochondrial disruption. Elevated levels of cardiac injury markers and oxidative stress indicators, such as CK-MB and LDH were observed. Evaluation via echocardiography within 2 h post-resuscitation revealed a marked decrease in EF and FS, indicating compromised contractile function, with some degree of recovery observed over time. Recent studies have shown that canagliflozin attenuates acute cardiac dysfunction after CPR in non-diabetic rats by improving markers of myocardial injury and decreasing the incidence of arrhythmias, but no morphological changes were observed.⁸ This difference may highlight the role of diabetes in exacerbating cardiac injury after resuscitation.

Diabetic myocardial I/RI is associated with autophagy dysfunction, which may constitute one of the underlying pathogenic mechanisms.²⁰ Autophagy, comprising double-membrane autophagosomes and lysosomes, serves as a cellular cleansing mechanism, degrading damaged organelles, and proteins to maintain cellular homeostasis. Under various stress conditions such as hyperglycemia, oxidative stress, and mitochondrial dysfunction, myocardial cells undergo H_2O_2 -mediated modification of Atg4 at Cys81, promoting the conversion of LC3B-I to LC3B-II and thus activating autophagy.^{21,22} Autophagy has a dual function in myocardial I/RI. During ischemia, upregulated autophagy exerts cardioprotective effects, but its sustained activation during reperfusion may exacerbate cellular damage.²³ In diabetic myocardial I/RI, excessive ROS production by damaged mitochondria leads to oxidative damage and drives autophagic cell death, which can be induced by degradation of essential cellular components and aberrant autophagic lysosomal degradation, and this overactivation of autophagy may be associated with multiple mechanisms. Studies suggest that in T2DM myocardial I/RI, autophagy is overactivated and accompanied by apoptosis. Inhibition of AMPK phosphorylation reduces the expression of LC3 II/I and thereby attenuates myocardial I/RI.²⁴ Furthermore, Chen et al. discovered an upregulation of HMGB1 following diabetic myocardial I/RI, which resulted in excessive autophagy activation and further aggravated myocardial injury.²⁵ Others like Guan have observed significantly increased calpain-1/2 activity in diabetic myocardial I/RI compared to non-diabetic counterparts, with degradation of Atg5 and LAMP2 resulting in increased autophagic flux and deteriorated cardiac function.²⁶ Following CA/CPR in T2DM rats, we observed a similar phenomenon of excessive autophagy. Studies on autophagy-deficient mice (cATG5^{-/-}) have demonstrated that decreased mitochondrial quality and function

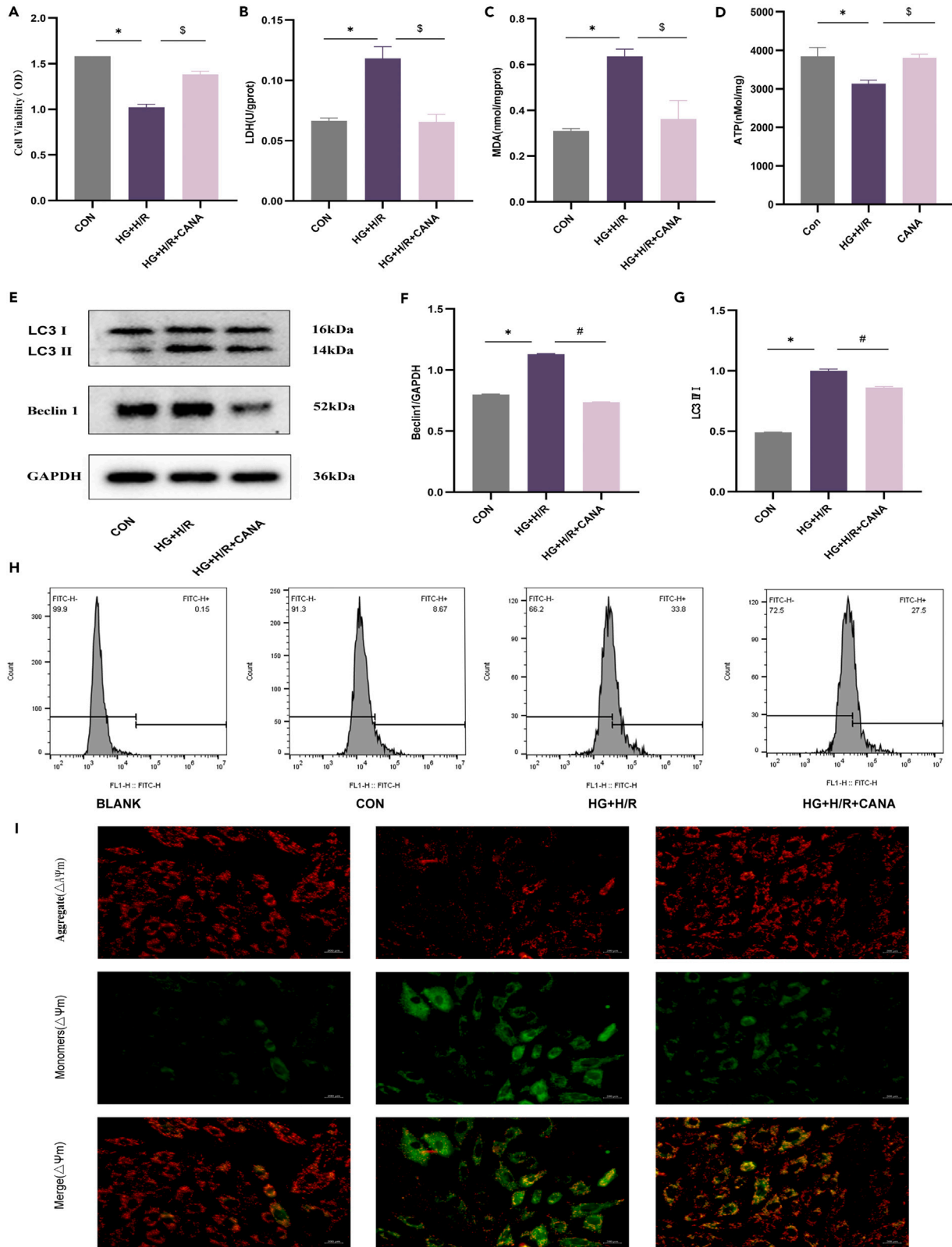


Figure 4. Canagliflozin improves HG + H/R injury in H9c2 cardiomyocytes

- (A) Viability of H9c2 cardiomyocytes between groups (n = 3).
(B) LDH activity in H9c2 cardiomyocytes between groups (n = 3).
(C) Malondialdehyde (MDA) content of H9c2 cardiomyocytes between groups (n = 3).
(D) ATP content of H9c2 cardiomyocytes between groups (n = 3).
(E) Representative protein bands for LC3II/I, Beclin 1, and GAPDH in H9c2 cardiomyocytes.
(F) Quantitative analysis of Beclin 1 protein expression level in H9c2 cardiomyocyte between groups (n = 3).
(G) Quantitative analysis of LC3II/I protein expression level in H9c2 cardiomyocyte between groups (n = 3).
(H) Effect of canagliflozin on reactive oxygen species (ROS) in H9c2 cardiomyocytes under high glucose (HG) + hypoxic-reoxygenation (H/R) injury conditions.
(I) Effect of canagliflozin on mitochondrial membrane potential (MMP) in H9c2 cardiomyocytes under HG + H/R injury conditions. Measurement data were presented as mean \pm SD. Differences among groups were determined by one-way ANOVA and LSD-test. * $p < 0.05$, CON versus HG + H/R group; [§] $p < 0.05$, HG + H/R versus HG + H/R + CANA group.

disrupts energy supply and calcium handling, resulting in reduced cardiac contractility. Furthermore, autophagy regulates the phosphorylation of troponin I, a critical protein in myofilament function essential for effective cardiac contraction under stress conditions.^{27–29} Following CA/CPR in T2DM rats, we observed similar excessive autophagy phenomena. Diabetic rats showed myocardial structural damage and increased autophagosomes after ROSC, with significantly elevated autophagy markers LC3 and Beclin1. Consequently, left ventricular systolic function (LVESV and LVD_s) and contractility (LVEF and LVFS) were markedly reduced and negatively correlated with autophagy protein levels. This observation is consistent with previous findings in patients with acute myocardial infarction where increased autophagic activity was negatively correlated with LVEF.³⁰ *In vitro*, LC3 II/I and Beclin 1 protein in cardiomyocytes significantly elevated, and Akt/mTOR expression was inhibited after HG and H/R. Activation of Akt/mTOR phosphorylation by canagliflozin effectively inhibited the formation of autophagic vesicles and the induction of autophagy proteins, which was accompanied by an increase in the expression of the oxidation product MDA activity, and attenuated the decrease in mitochondrial membrane potential, thus improving cardiac function.

Previous research has indicated the protective value of SGLT-2i in diabetic myocardial I/RI. For instance, empagliflozin activates the JAK2/STAT3 pathway and downregulates the levels of Bax, Bcl-2, GRP78, and p-eIF-2 proteins, which diminishes cell apoptosis and excessive endoplasmic reticulum stress (ERS), thereby protecting cardiomyocytes from HG + H/R damage.³¹ Pretreatment with dapagliflozin significantly modulates OPA1 expression in HG + H/R-induced myocardial injury. It impedes the conversion of long-chain OPA1 to short-chain OPA1, promoting mitosis and autophagy levels, thereby notably alleviating mitochondrial damage. Further investigations revealed that dapagliflozin enhances p-AMPK/AMPK expression and suppresses mTOR phosphorylation, activating OPA1-mediated mitochondrial autophagy, thus mitigating HG and H/R-induced myocardial injury.³² Moreover, dapagliflozin regulates the expression of eNOS and iNOS, inhibits cardiac lipid peroxidation and protects diabetic rat hearts from myocardial I/R injury.³³ Empagliflozin and dapagliflozin are highly selective SGLT2 inhibitors, whereas canagliflozin is a less selective SGLT2 inhibitor targeting both SGLT1 and SGLT2. Previous studies have demonstrated that SGLT1 is uniformly expressed throughout the myocardium, and its inhibition can mitigate myocardial damage exacerbated by high glucose levels during reperfusion.^{34,35} The administration of canagliflozin offers some protection against diabetic myocardial I/RI, however, the exact mechanisms underlying its protective effects remain incompletely understood. Research by Qin et al. demonstrates that inhibiting cardiomyocyte autophagy by activating the PI3K/Akt/mTOR pathway may protect against myocardial I/RI.³⁶ During acute I/RI, increased phosphorylation of myocardial ROS and insulin receptor substrate 1 serine residues impairs their binding ability to PI3K/Akt, thereby weakening myocardial self-protection. Our study confirmed similar outcomes in myocardium subjected to HG and H/R treatments. We observed a significant decrease in the expression of p-Akt/Akt and p-mTOR/mTOR in myocardial cells under these conditions. Conversely, Akt/mTOR phosphorylation levels were found to be activated by pretreatment with canagliflozin. Using the PI3K-specific inhibitor Ly294002 further validated the link between canagliflozin and the PI3K/Akt/mTOR pathway. Our observations suggest that Ly294002 attenuates the autophagic and cardioprotective effects of reoxygenated canagliflozin after reoxygenation.

Our study provides evidence that canagliflozin alleviates PRMD in T2DM rats after resuscitation. The potential cardioprotective role of canagliflozin may be mediated through regulation of the PI3K/Akt/mTOR pathway and myocardial autophagy. These findings provide valuable insights into the potential cardiovascular benefits of canagliflozin after resuscitation.

Limitations of the study

Our study has several limitations. Firstly, CA model effectively represents the etiology of most CA, but it cannot cover other clinically less common causes of CA; Secondly, our observation period was limited to 6 h without survival study. Future research should focus on extended prognosis monitoring. Thirdly, the study was limited to a single time point observation of autophagy. More comprehensive future research is needed to explore the dynamic changes in autophagic flux. Finally, our study was unable to fully elucidate the extent of the association between the cardioprotective effects of canagliflozin and its glycemic benefits, which highlights the need for additional basic and clinical research to clarify this association.

STAR★METHODS

Detailed methods are provided in the online version of this paper and include the following:

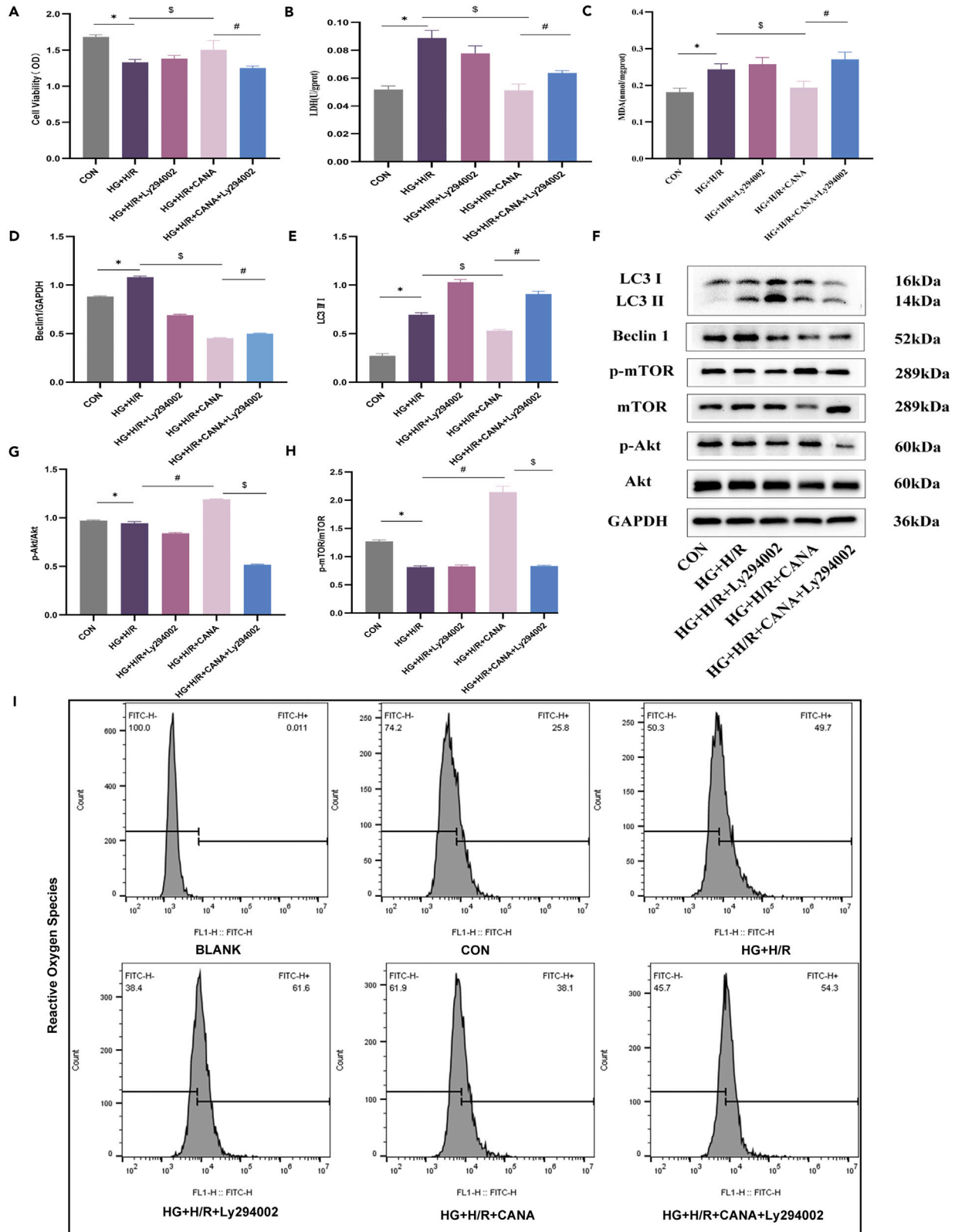


Figure 5. Canagliflozin inhibits autophagy through PI3K/Akt/mTOR pathway

(A) Viability of H9c2 cardiomyocytes between groups (n = 3).
(B) LDH activity in H9c2 cardiomyocytes between groups (n = 3).
(C) MDA content of H9c2 cardiomyocytes between groups (n = 3).
(D) Quantitative analysis of Beclin 1 protein expression level in H9c2 cardiomyocytes (n = 3).
(E) Quantitative analysis of LC3II/I protein expression level in H9c2 cardiomyocytes (n = 3).
(F) Representative protein bands for LC3II/I, Beclin 1, and p-mTOR, mTOR, p-Akt, Akt, and GAPDH in H9c2 cardiomyocytes.
(G) Quantitative analysis of p-Akt/Akt protein expression level in H9c2 cardiomyocytes (n = 3).
(H) Quantitative analysis of p-mTOR/mTOR protein expression level in H9c2 cardiomyocytes (n = 3).
(I) Ly294002 reduces the effect of canagliflozin on ROS in H9c2 cardiomyocytes with HG + H/R injury. Measurement data were presented as mean ± SD. Differences among groups were determined by one-way ANOVA and LSD-test. *p < 0.05, CON versus HG + H/R group; #p < 0.05, HG + H/R versus HG + H/R + CANA group; §p < 0.05, HG + H/R + CANA versus HG + H/R+CANA+Ly294002 group.

- [KEY RESOURCES TABLE](#)
- [RESOURCE AVAILABILITY](#)
 - Lead contact
 - Materials availability
 - Data and code availability
- [EXPERIMENTAL MODEL AND STUDY PARTICIPANT DETAILS](#)
 - Animals
 - Cell
- [METHOD DETAILS](#)
 - Model of T2DM
 - Model of CA/CPR
 - Cell culture and treatments
 - Echocardiography
 - CK-MB and LDH measurement
 - Hematoxylin and eosin (H&E) staining
 - Transmission electron microscopy (TEM)
 - ATP measurement
 - ROS detection
 - MMP measurement
 - Western blotting
- [QUANTIFICATION AND STATISTICAL ANALYSIS](#)

ACKNOWLEDGMENTS

This work was supported by the National Natural Science Foundation of China (no. 82072134), the Research Fund of Anhui Institute of translational medicine (no.2023zhyx-C64 and 2022zhyx-C76), the Basic and Clinical Enhancement Project of Anhui Medical University (no.2019xkjT028 and 2023xkjT042), the Postgraduate Innovation Research and Practice Program of Anhui Medical University (no. YJS20230133 and YJS20230085), Anhui Province Key Research and Development Plan High-tech Special Project (no. 202304a05020071), Anhui University Excellent Young Talents Support Plan (no. gxyqZD2018026).

AUTHOR CONTRIBUTIONS

Conceptualization, Y.M.; methodology, H.T.F.; software, H.Y.; validation, Z.Y.J. and H.Y.; formal analysis, Z.L.L.; investigation, S.W. and L.B.R.; resources, X.W.Y.; data curation, H.Q.H., S.W., and W.M.J.; writing-original draft, H.Q.H.; writing-review editing, Y.M., H.T.F., and H.Q.H.; visualization, S.W., Z.Y.J., and P.S.N.; supervision, Y.M., H.T.F., W.M.J., and Z.H.Q.; project administration, Y.M. and H.T.F.; funding acquisition, Y.M., H.T.F., X.W.Y., H.Q.H., Z.Y.J., and Z.H.Q.

DECLARATION OF INTERESTS

The authors declare no competing interests.

Received: March 16, 2024

Revised: June 3, 2024

Accepted: June 28, 2024

Published: July 1, 2024

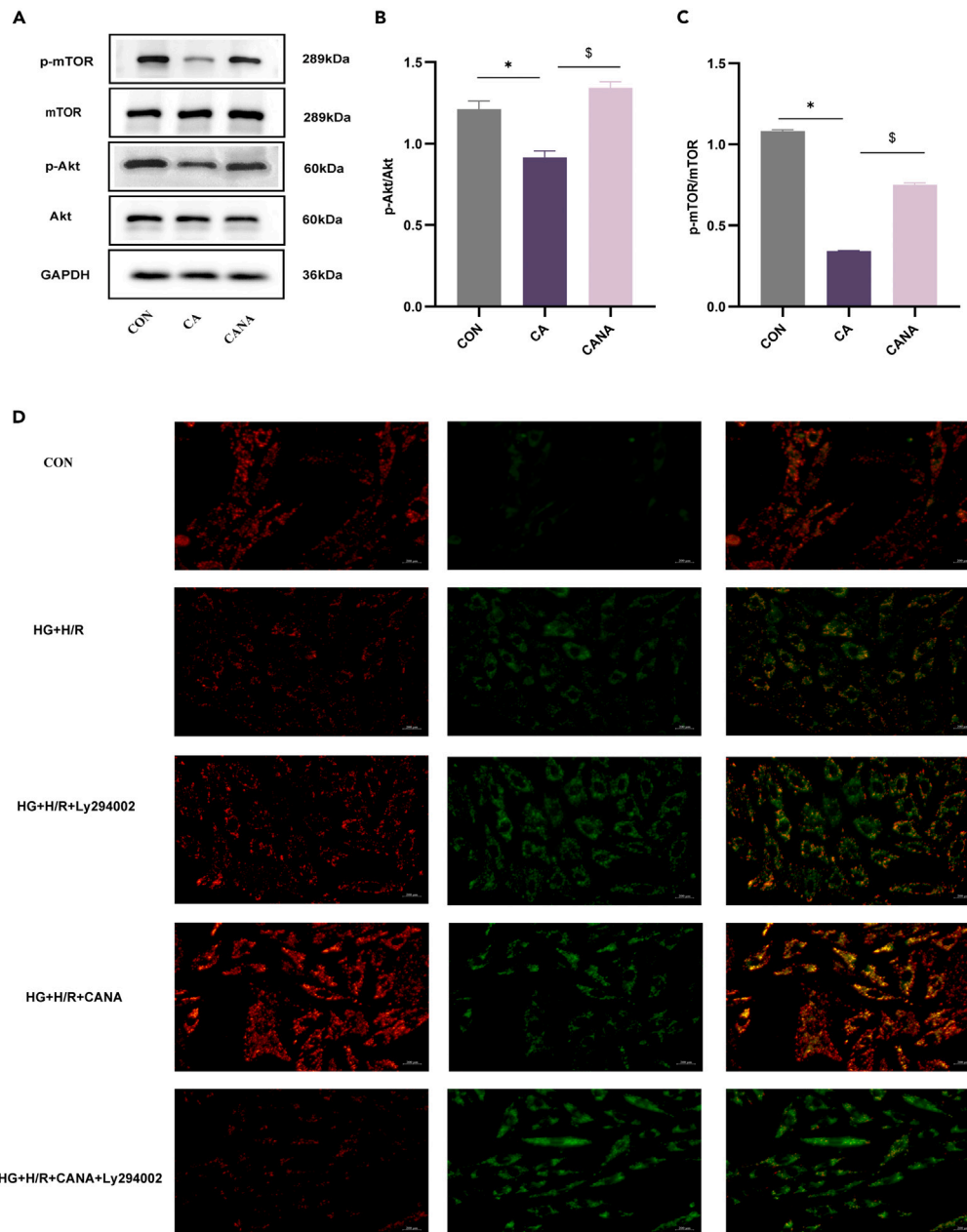


Figure 6. Canagliflozin inhibits myocardial tissue PI3K/Akt/mTOR pathway and attenuates Ly294002-induced mitochondrial membrane potential levels in cardiomyocytes

(A) Representative protein bands for p-mTOR, mTOR, p-Akt, Akt, and GAPDH in myocardial tissue.

(B) Quantitative analysis of p-Akt/Akt protein expression level in myocardial tissue ($n = 3$).

(C) Quantitative analysis of p-mTOR/mTOR protein expression level in myocardial tissue ($n = 3$).

(D) Ly294002 reduces the effect of canagliflozin on MMP in H9c2 cardiomyocytes with HG + H/R injury.

Measurement data were presented as mean \pm SD. Differences among groups were determined by one-way ANOVA and LSD-test. * $p < 0.05$, CON versus CA group; $^{\$}p < 0.05$, CA versus CANA group.

REFERENCES

- Sun, H., Saeedi, P., Karuranga, S., Pinkepank, M., Ogurtsova, K., Duncan, B.B., Stein, C., Basit, A., et al. (2022). IDF Diabetes Atlas: Global, regional and country-level diabetes prevalence estimates for 2021 and projections for 2045. *Diabetes Res. Clin. Pract.* 183, 109119. <https://doi.org/10.1016/j.diabres.2021.109119>.
- Tan, H.L., van Dongen, L.H., and Zimmerman, D.S. (2020). Sudden cardiac death in young patients with diabetes: a call to study additional causes beyond ischaemic heart disease. *Eur. Heart J.* 41,

- 2707–2709. <https://doi.org/10.1093/eurheartj/ehaa011>.
- Mohr, G.H., Søndergaard, K.B., Pallisgaard, J.L., Møller, S.G., Wissenberg, M., Karlsson, L., Hansen, S.M., Kragholm, K., Køber, L., Lippert, F., et al. (2020). Survival of patients with and without diabetes following out-of-hospital cardiac arrest: A nationwide Danish study. *Eur. Heart J. Acute Cardiovasc. Care* 9, 599–607. <https://doi.org/10.1177/2048872618823349>.
 - Nehme, Z., Nair, R., Andrew, E., Bernard, S., Lijovic, M., Villani, M., Zoungas, S., and Smith, K. (2016). Effect of diabetes and pre-hospital blood glucose level on survival and recovery after out-of-hospital cardiac arrest. *Crit. Care Resusc.* 18, 69–77.
 - Perkovic, V., de Zeeuw, D., Mahaffey, K.W., Fulcher, G., Erondou, N., Shaw, W., Barrett, T.D., Weidner-Wells, M., Deng, H., Matthews, D.R., and Neal, B. (2018). Canagliflozin and renal outcomes in type 2 diabetes: results from the CANVAS Program randomised clinical trials. *Lancet Diabetes Endocrinol.* 6, 691–704. [https://doi.org/10.1016/S2213-8587\(18\)30141-4](https://doi.org/10.1016/S2213-8587(18)30141-4).
 - Zinman, B., Wanner, C., Lachin, J.M., Fitchett, D., Bluhmki, E., Hantel, S., Mattheus, M., Devins, T., Johansen, O.E., Woerle, H.J., et al. (2015). Empagliflozin, Cardiovascular Outcomes, and Mortality in Type 2 Diabetes. *N. Engl. J. Med.* 373, 2117–2128. <https://doi.org/10.1056/NEJMoa1504720>.
 - Vaduganathan, M., Docherty, K.F., Claggett, B.L., Jhund, P.S., de Boer, R.A., Hernandez, A.F., Inzucchi, S.E., Kosiborod, M.N., Lam, C.S.P., Martinez, F., et al. (2022). SGLT-2 inhibitors in patients with heart failure: a comprehensive meta-analysis of five randomised controlled trials. *Lancet* 400, 757–767. [https://doi.org/10.1016/S0140-6736\(22\)01429-5](https://doi.org/10.1016/S0140-6736(22)01429-5).
 - Ju, F., Abbott, G.W., Li, J., Wang, Q., Liu, T., Liu, Q., and Hu, Z. (2024). Canagliflozin Pretreatment Attenuates Myocardial Dysfunction and Improves Postcardiac Arrest Outcomes After Cardiac Arrest and Cardiopulmonary Resuscitation in Mice. *Cardiovasc. Drugs Ther.* 38, 279–295. <https://doi.org/10.1007/s10557-022-07419-8>.
 - Liu, Y.-Y., Sun, C., Xue, F.-S., Yang, G.-Z., Li, H.-X., Liu, Q., and Liao, X. (2018). Effect of Autophagy Inhibition on the Protection of Ischemia Preconditioning against Myocardial Ischemia/Reperfusion Injury in Diabetic Rats. *Chin. Med. J.* 131, 1702–1709. <https://doi.org/10.4103/0366-6999.235867>.
 - Lu, R., Wei, Z., Wang, Z., Xu, S., Sun, K., Cheng, P., Huang, X., You, H., Guo, F., Liang, S., and Chen, A.M. (2023). Mulberroside A alleviates osteoarthritis via restoring impaired autophagy and suppressing MAPK/NF-κB/PI3K-AKT-mTOR signaling pathways. *iScience* 26, 105936. <https://doi.org/10.1016/j.isci.2023.105936>.
 - Bhardwaj, A., Alwakeel, M., Duggal, A., Fadel, F.A., and Abella, B.S. (2022). Post resuscitation myocardial dysfunction and echocardiographic characteristics following COVID-19 cardiac arrest. *Resuscitation* 173, 57–58. <https://doi.org/10.1016/j.resuscitation.2022.02.009>.
 - Ponikowski, P., Voors, A.A., Anker, S.D., Bueno, H., Cleland, J.G.F., Coats, A.J.S., Falk, V., González-Juanatey, J.R., Harjola, V.-P., Jankowska, E.A., et al. (2016). 2016 ESC Guidelines for the diagnosis and treatment of acute and chronic heart failure: The Task Force for the diagnosis and treatment of acute and chronic heart failure of the European Society of Cardiology (ESC) Developed with the special contribution of the Heart Failure Association (HFA) of the ESC. *Eur. Heart J.* 37, 2129–2200. <https://doi.org/10.1093/eurheartj/ehw128>.
 - Lazzarin, T., Tonon, C.R., Martins, D., Fávero, E.L., Baumgratz, T.D., Pereira, F.W.L., Pinheiro, V.R., Ballarin, R.S., Queiroz, D.A.R., Azevedo, P.S., et al. (2022). Post-Cardiac Arrest: Mechanisms, Management, and Future Perspectives. *J. Clin. Med.* 12, 259. <https://doi.org/10.3390/jcm12010259>.
 - Samidurai, A., Ockaili, R., Cain, C., Roh, S.K., Filippone, S.M., Kraskauskas, D., Kukreja, R.C., and Das, A. (2020). Differential Regulation of mTOR Complexes with miR-302a Attenuates Myocardial Reperfusion Injury in Diabetes. *iScience* 23, 101863. <https://doi.org/10.1016/j.isci.2020.101863>.
 - Das, A., Salloum, F.N., Filippone, S.M., Durrant, D.E., Rokosh, G., Bolli, R., and Kukreja, R.C. (2015). Inhibition of mammalian target of rapamycin protects against reperfusion injury in diabetic heart through STAT3 signaling. *Basic Res. Cardiol.* 110, 31. <https://doi.org/10.1007/s00395-015-0486-5>.
 - Yang, T., and Zhang, D. (2023). Research progress on the effects of novel hypoglycemic drugs in diabetes combined with myocardial ischemia/reperfusion injury. *Ageing Res. Rev.* 86, 101884. <https://doi.org/10.1016/j.arr.2023.101884>.
 - Mahalakshmi, A., and Kurian, G.A. (2018). Evaluating the impact of diabetes and diabetic cardiomyopathy rat heart on the outcome of ischemia-reperfusion associated oxidative stress. *Free Radic. Biol. Med.* 118, 35–43. <https://doi.org/10.1016/j.freeradbiomed.2018.02.021>.
 - Xiang, M., Lu, Y., Xin, L., Gao, J., Shang, C., Jiang, Z., Lin, H., Fang, X., Qu, Y., Wang, Y., et al. (2021). Role of Oxidative Stress in Reperfusion following Myocardial Ischemia and Its Treatments. *Oxid. Med. Cell. Longev.* 2021, 6614009. <https://doi.org/10.1155/2021/6614009>.
 - Lejay, A., Fang, F., John, R., Van, J.A.D., Barr, M., Thaveau, F., Chakfe, N., Geny, B., and Scholey, J.W. (2016). Ischemia reperfusion injury, ischemic conditioning and diabetes mellitus. *J. Mol. Cell. Cardiol.* 91, 11–22. <https://doi.org/10.1016/j.yjmcc.2015.12.020>.
 - Zhang, D., He, Y., Ye, X., Cai, Y., Xu, J., Zhang, L., Li, M., Liu, H., Wang, S., and Xia, Z. (2020). Activation of autophagy inhibits nucleotide-binding oligomerization domain-like receptor protein 3 inflammasome activation and attenuates myocardial ischemia-reperfusion injury in diabetic rats. *J. Diabetes Investig.* 11, 1126–1136. <https://doi.org/10.1111/jdi.13235>.
 - Yun, H.R., Jo, Y.H., Kim, J., Shin, Y., Kim, S.S., and Choi, T.G. (2020). Roles of Autophagy in Oxidative Stress. *Int. J. Mol. Sci.* 21, 3289. <https://doi.org/10.3390/ijms21093289>.
 - Scherz-Shouval, R., Shvets, E., Fass, E., Shorer, H., Gil, L., and Elazar, Z. (2007). Reactive oxygen species are essential for autophagy and specifically regulate the activity of Atg4. *EMBO J.* 26, 1749–1760. <https://doi.org/10.1038/sj.emboj.7601623>.
 - Xing, Y., Sui, Z., Liu, Y., Wang, M.-M., Wei, X., Lu, Q., Wang, X., Liu, N., Lu, C., Chen, R., et al. (2022). Blunting TRPML1 channels protects myocardial ischemia/reperfusion injury by restoring impaired cardiomyocyte autophagy. *Basic Res. Cardiol.* 117, 20. <https://doi.org/10.1007/s00395-022-00930-x>.
 - Wang, S., Wang, C., Yan, F., Wang, T., He, Y., Li, H., Xia, Z., and Zhang, Z. (2017). N-Acetylcysteine Attenuates Diabetic Myocardial Ischemia Reperfusion Injury through Inhibiting Excessive Autophagy. *Mediators Inflamm.* 2017, 9257291. <https://doi.org/10.1155/2017/9257291>.
 - Chen, C., Lu, C., He, D., Na, N., Wu, Y., Luo, Z., and Huang, F. (2021). Inhibition of HMGB1 alleviates myocardial ischemia/reperfusion injury in diabetic mice via suppressing autophagy. *Microvasc. Res.* 138, 104204. <https://doi.org/10.1016/j.mvr.2021.104204>.
 - Guan, L., Yu, Z., Che, Z., Zhang, H., Yu, Y., Yang, D., Qian, D., Chen, R., and Yu, M. (2023). Experimental diabetes exacerbates autophagic flux impairment during myocardial I/R injury through calpain-mediated cleavage of Atg5/LAMP2. *J. Cell Mol. Med.* 27, 232–245. <https://doi.org/10.1111/jcmm.17642>.
 - Chi, R.-F., Wang, J.-P., Wang, K., Zhang, X.-L., Zhang, Y.-A., Kang, Y.-M., Han, X.-B., Li, B., Qin, F.-Z., and Fan, B.-A. (2017). Progressive Reduction in Myocyte Autophagy After Myocardial Infarction in Rabbits: Association with Oxidative Stress and Left Ventricular Remodeling. *Cell. Physiol. Biochem.* 44, 2439–2454. <https://doi.org/10.1159/000486167>.
 - Ljubojević-Holzer, S., Kraler, S., Djalalinac, N., Abdellatif, M., Voglhuber, J., Schipke, J., Schmidt, M., Kling, K.-M., Franke, G.T., Herbst, V., et al. (2022). Loss of autophagy protein ATG5 impairs cardiac capacity in mice and humans through diminishing mitochondrial abundance and disrupting Ca²⁺ cycling. *Cardiovasc. Res.* 118, 1492–1505. <https://doi.org/10.1093/cvr/cvab112>.
 - Fajardo, G., Coronado, M., Matthews, M., and Bernstein, D. (2022). Mitochondrial Quality Control in the Heart: The Balance between Physiological and Pathological Stress. *Biomedicines* 10, 1375. <https://doi.org/10.3390/biomedicines10061375>.
 - Kong, M.G., Suh, J., Cho, Y.H., Lee, N.H., and Park, H.W. (2022). Autophagy biomarkers in patients with acute myocardial infarction. *Eur. Heart J.* 43, ehac544.1276. <https://doi.org/10.1093/eurheartj/ehac544.1276>.
 - Zhang, F., Cao, X., Zhao, C., Chen, L., and Chen, X. (2023). Empagliflozin activates JAK2/STAT3 signaling and protects cardiomyocytes from hypoxia/reoxygenation injury under high glucose conditions. *J. Thromb. Thrombolysis* 55, 116–125. <https://doi.org/10.1007/s11239-022-02719-0>.
 - Tu, W., Li, L., Yi, M., Chen, J., Wang, X., and Sun, Y. (2023). Dapagliflozin attenuates high glucose- and hypoxia/reoxygenation-induced injury via activating AMPK/mTOR-OPA1-mediated mitochondrial autophagy in H9c2 cardiomyocytes. *Arch. Physiol. Biochem.* 1–11. <https://doi.org/10.1080/13813455.2023.2252200>.
 - Xiong, S., Mo, D., Wu, Y., Wu, P., Hu, Y., and Gong, F. (2023). The effect of dapagliflozin on myocardial ischemia-reperfusion injury in diabetic rats. *Can. J. Physiol. Pharmacol.* 101, 80–89. <https://doi.org/10.1139/cjpp-2022-0045>.
 - Lim, V.G., Bell, R.M., Arjun, S., Kolatsi-Joannou, M., Long, D.A., and Yellon, D.M. (2019). SGLT2 Inhibitor, Canagliflozin, Attenuates Myocardial Infarction in the Diabetic and Nondiabetic Heart. *JACC. Basic Transl. Sci.* 4, 15–26. <https://doi.org/10.1016/j.jacbs.2018.10.002>.

35. Rieg, T., and Vallon, V. (2018). Development of SGLT1 and SGLT2 inhibitors. *Diabetologia* 61, 2079–2086. <https://doi.org/10.1007/s00125-018-4654-7>.
36. Qin, G.-W., Lu, P., Peng, L., and Jiang, W. (2021). Ginsenoside Rb1 Inhibits Cardiomyocyte Autophagy via PI3K/Akt/mTOR Signaling Pathway and Reduces Myocardial Ischemia/Reperfusion Injury. *Am. J. Chin. Med.* 49, 1913–1927. <https://doi.org/10.1142/S0192415X21500907>.
37. Xiao, Y., Su, C., Zhang, G., Liang, L., Jin, T., Bradley, J., Ornato, J.P., and Tang, W. (2022). Vitamin C Improves the Outcomes of Cardiopulmonary Resuscitation and Alters Shedding of Syndecan-1 and p38/MAPK Phosphorylation in a Rat Model. *J. Am. Heart Assoc.* 11, e023787. <https://doi.org/10.1161/JAHA.121.023787>.
38. Sun, M., Mao, S., Wu, C., Zhao, X., Guo, C., Hu, J., Xu, S., Zheng, F., Zhu, G., Tao, H., et al. (2024). Piezo1-Mediated Neurogenic Inflammatory Cascade Exacerbates Ventricular Remodeling After Myocardial Infarction. *Circulation* 149, 1516–1533. <https://doi.org/10.1161/CIRCULATIONAHA.123.065390>.
39. Gheibi, S., Kashfi, K., and Ghasemi, A. (2017). A practical guide for induction of type-2 diabetes in rat: Incorporating a high-fat diet and streptozotocin. *Biomed. Pharmacother.* 95, 605–613. <https://doi.org/10.1016/j.biopha.2017.08.098>.
40. Xie, S., Zhang, M., Shi, W., Xing, Y., Huang, Y., Fang, W.-X., Liu, S.-Q., Chen, M.-Y., Zhang, T., Chen, S., et al. (2022). Long-Term Activation of Glucagon-like peptide-1 receptor by Dulaglutide Prevents Diabetic Heart Failure and Metabolic Remodeling in Type 2 Diabetes. *J. Am. Heart Assoc.* 11, e026728. <https://doi.org/10.1161/JAHA.122.026728>.
41. Reagan-Shaw, S., Nihal, M., and Ahmad, N. (2008). Dose translation from animal to human studies revisited. *FASEB J.* 22, 659–661. <https://doi.org/10.1096/fj.07-9574LSF>.
42. Cui, Y., Li, Y., Guo, C., Li, Y., Ma, Y., and Dong, Z. (2022). Pharmacokinetic Interactions between Canagliflozin and Sorafenib or Lenvatinib in Rats. *Molecules* 27, 5419. <https://doi.org/10.3390/molecules27175419>.
43. Yang, M., Hua, T., Yang, Z., Chen, L., Zou, Y., Huang, X., and Li, J. (2020). The Protective Effect of rhBNP on Postresuscitation Myocardial Dysfunction in a Rat Cardiac Arrest Model. *BioMed Res. Int.* 2020, 6969053. <https://doi.org/10.1155/2020/6969053>.
44. Kondo, H., Akoumianakis, I., Badi, I., Akawi, N., Kotanidis, C.P., Polkinghorne, M., Stadiotti, I., Sommariva, E., Antonopoulos, A.S., Carena, M.C., et al. (2021). Effects of canagliflozin on human myocardial redox signalling: clinical implications. *Eur. Heart J.* 42, 4947–4960. <https://doi.org/10.1093/eurheartj/ehab420>.
45. Iijima, H., Kifuji, T., Maruyama, N., and Inagaki, N. (2015). Pharmacokinetics, Pharmacodynamics, and Safety of Canagliflozin in Japanese Patients with Type 2 Diabetes Mellitus. *Adv. Ther.* 32, 768–782. <https://doi.org/10.1007/s12325-015-0234-0>.
46. Li, L., Zhou, Y., Li, Y., Wang, L., Sun, L., Zhou, L., Arai, H., Qi, Y., and Xu, Y. (2017). Aqueous extract of Cortex Dictamni protects H9c2 cardiomyocytes from hypoxia/reoxygenation-induced oxidative stress and apoptosis by PI3K/Akt signaling pathway. *Biomed. Pharmacother.* 89, 233–244. <https://doi.org/10.1016/j.biopha.2017.02.013>.
47. Schiattarella, G.G., Altamirano, F., Tong, D., French, K.M., Villalobos, E., Kim, S.Y., Luo, X., Jiang, N., May, H.I., Wang, Z.V., et al. (2019). Nitrosative Stress Drives Heart Failure with Preserved Ejection Fraction. *Nature* 568, 351–356. <https://doi.org/10.1038/s41586-019-1100-z>.

STAR★METHODS

KEY RESOURCES TABLE

REAGENT or RESOURCE	SOURCE	IDENTIFIER
Antibodies		
Phospho-Akt (Ser473) (D9E) XP® Rabbit mAb	Cell Signaling Technology, USA	Cat#4060; RRID: AB_2315049
Akt (pan) (C67E7) Rabbit mAb	Cell Signaling Technology, USA	Cat#4691; RRID: AB_915783
Phospho-mTOR (Ser2448) (D9C2) XP® Rabbit mAb	Cell Signaling Technology, USA	Cat#5536; RRID: AB_10691552
mTOR (7C10) Rabbit mAb	Cell Signaling Technology, USA	Cat#2983 RRID: AB_2105622
LC3 Polyclonal antibody	proteintech, USA	Cat#14600-1-AP; RRID: AB_2137737
Beclin 1 Monoclonal antibody	proteintech, USA	Cat#66665-1-Ig; RRID: AB_2882020
Anti-GAPDH antibody [EPR16891]	Abcam plc, UK	Cat#ab181602; RRID: AB_2630358
Goat Anti-Rabbit IgG (H+L) HRP	Affinity Biosciences, USA	Cat# S0001; RRID: AB_2839429
Goat Anti-Mouse IgG (H+L) HRP	Affinity Biosciences, USA	Cat# S0002; RRID: AB_2839430
Chemicals, peptides, and recombinant proteins		
Canagliflozin- <i>in vivo</i>	Janssen Ortho Llc, USA	TV-FRM-60395
Canagliflozin- <i>in vitro</i>	Selleck Chemicals	S2760, CAS: 842133-18-0
Streptomycin	Sigma-Aldrich	S6501, CAS:3810-74-0
Ly294002	APExBIO Technology	A8250, AS:154447-36-6
Critical commercial assays		
CK-MB ELISA Kit	Elabscience Biotechnology, China	E-EL-R1327
LDH ELISA Kit	Cloud-Clone Corp., China	SEB864Ra
Enhanced ATP Assay Kit	Beyotime Biotechnology, China	S0027
Mitochondrial membrane potential assay kit with JC-1	Beyotime Biotechnology, China	C2006
Reactive Oxygen Species Assay Kit	Beyotime Biotechnology, China	S0033
Malondialdehyde assay kit	Nanjing Jiancheng Bioengineering Institute, China	A003-1
Experimental models: Cell lines		
H9c2(2-1)	Pricella, Wuhan, China	CL-0089
Experimental models: Organisms/strains		
SD-rats	Jinan Pengyue Laboratory Animal Breeding Co Ltd in Jinan, Shandong, China	No.370726220100737187
High Fat Diets	Jiangsu Xietong Pharmaceutical Bio-engineering Co., Ltd.	D12451
Software and algorithms		
Image J 1.53	National Institutes of Health	https://image.nih.gov/ij/
FlowJo	FlowJo Software	https://www.flowjo.com/
GraphPad Prism v9.5.1	GraphPad Software	v9.5.1
G*Power	*Power software	Version 3.1.9.7

RESOURCE AVAILABILITY

Lead contact

Please contact the lead contact person, Min Yang (yangmin@ahmu.edu.cn), for further information and resource requests.

Materials availability

This study did not generate new unique reagents.

Data and code availability

All data produced in this study are included in the published article.

This work does not report original code.

No original code is reported in this paper. Any information needed to re-analyze the data reported in this paper is available upon request from the primary contact.

EXPERIMENTAL MODEL AND STUDY PARTICIPANT DETAILS

Animals

Animal manipulations adhered to the guidelines of the Ethics Committee for Laboratory Animals of Anhui Medical University and the Centre for Laboratory Animal Research of Anhui Medical University (Approval No. 20200383). Approval from the Shandong Provincial Laboratory Animal Centre was obtained to utilize male SD-Dawley rats from Jinan Pengyue Laboratory Animal Breeding Co Ltd in Jinan, Shandong, China. The rats weighed (250~300) g and were 10 weeks old. The rats were able to freely consume food and water. Rats were kept under constant conditions of temperature (22 ± 2) °C and relative humidity ($60 \pm 5\%$). Sample size determination was based on previous literature, the complexity of model construction, and preliminary experimental results from echocardiographic measurements of the rats' left ventricular function data. Expected power was set at 0.8 ($1-\beta$) with a significance level (α) of 0.05 using G*Power.^{37,38}

Cell

H9c2 cardiomyocytes were purchased from Procell Life Sciences Ltd. Cells were identified to species, DNA was extracted from the sample, and an appropriate amount of sample DNA was used to amplify the animal mitochondrial COI gene using the species-specific fluorescent compound primer MX, and the amplified product was detected and analyzed by capillary electrophoresis on the GenReader 7010 instrument. The cellular DNA amplification profile was clear, the internal reference gene position, amplification peaks were normal, the rat species-specific primer position showed specific peaks, and no amplification peaks were seen at other species-specific primer positions. The cell samples were determined to be rat cells and no DNA contamination from other species was seen. No mycoplasma contamination was detected.

METHOD DETAILS

Model of T2DM

Rats were acclimatized and nourished for one week prior to an eight-week high-fat dietary (HFD) intervention. Following overnight fasting, a Streptozotocin (STZ) solution (30 mg/kg) was administered intraperitoneally.³⁹ Fasting blood glucose (FBG) was collected from the tail vein after 72 hours. FBG were assessed 72 hours post-STZ injection and monitored for over one week. FBG level of ≥ 11.1 mmol/L or random blood glucose levels exceeding 16.7 mmol/L confirmed the successful establishment of the T2DM model.⁴⁰ Failure to meet the criteria even after the reinjection was considered a modeling failure. T2DM model was further evaluated using glucose and insulin tolerance tests. These tests involved intraperitoneal injections of glucose at 1 g/kg and insulin at 1.0 U/kg, followed by plotting blood glucose curves over various time intervals. Rats were randomly assigned to three groups: a control group (CON), a group that underwent CA/CPR (CA), and a group that underwent CA/CPR and received canagliflozin at a dose of 10mg/kg/day via gavage for four weeks (CANA).^{41,42} The CON and CA groups were concurrently administered an equivalent volume of saline solution for the same duration.

Model of CA/CPR

Male rats fasted overnight with water access, anesthesia was administered with CO₂ and pentobarbital (45mg/kg).⁴³ Subsequently, rats were intubated via trachea and ventilated with a KW-100-2 ventilator (Nanjing Kelvin Biotechnology Co., Ltd, China) at 6.5 ml/kg tidal volume and 100 breaths/min. Electrocardiograms were recorded via subcutaneous limb electrodes, while a heat lamp maintained their body temperature at 36.5 ± 0.5 °C. For hemodynamic measurement and fluid replacement, a PE-50 catheter was inserted into the left inguinal arteriovenous system. Sterile acupuncture needles were used as an electrode to locate points A and B and insert into the epicardium to induce fibrillation. The specific insertion point was determined according to the anatomic characteristics of rats, point A corresponds to the most intense apical pulsation, point B is located 2cm parallel to the right of point A, with an insertion depth of 1.5-2.0 cm.

Under continuous monitoring of blood pressure and electrocardiographic changes, ventricular fibrillation was induced using 0.5 mA electrical stimulation for 3 minutes, with the current not exceeding 1 mA. Six minutes after the onset of ventricular fibrillation, chest compressions were administered at a rate of 200 compressions per minute, with a depth of 1.0-1.3 cm, for a duration of 8 minutes. Following the compressions, defibrillation was performed using a 4J shock, up to a maximum of three attempts. Return of spontaneous circulation (ROSC) was

considered achieved if the mean arterial pressure (MAP) was ≥ 50 mmHg and sustained for 5 minutes. During compressions, epinephrine (1 mg/kg) was administered as needed. After achieving ROSC, the rats' vital signs were monitored for 6 hours. For subsequent analysis, the rats' hearts and serum were rapidly preserved at -80°C after the 6-hour monitoring period.

Cell culture and treatments

H9c2 cardiomyocytes were cultured in medium supplemented with fetal bovine serum and penicillin-streptomycin antibiotics, and maintained at 37 degrees constant temperature with 5% CO_2 . We conducted three independent *in vitro* experiments, each repeated three times, to ensure robustness and consistency. Experiment 1 aimed to determine optimal high glucose (HG) concentration and growth duration for H9c2 cells. A glucose gradient (5.56 mmol/L to 100.00 mmol/L) was applied for 24, 48, and 96 hours of cell culture, followed by 12 hours of hypoxia (95% N_2 , 5% CO_2) and 4 hours of reoxygenation. Experiment 2 aimed to examine the impact of canagliflozin preconditioning on cardiomyocytes under HG and hypoxia/reoxygenation (H/R) conditions. Experiment 3 introduced the PI3K/Akt pathway inhibitor, Ly294002, at a concentration of 10 $\mu\text{mol/L}$. The concentration and duration of action of Canagliflozin and Ly294002 were determined based on pharmacokinetics and previous studies in the literature.⁴⁴⁻⁴⁶ Groupings are detailed in Figure 1 to maintain consistency and credibility throughout the study.

Echocardiography

Cardiac function in rats was evaluated using a high-resolution echocardiography system (VINNO6 LAB, VINNO Technology, China). M-mode images were captured from the parasternal long-axis view, guided by two-dimensional echocardiography. Left ventricular end-systolic volume (LVESV), left ventricular end-systolic dimension (LVDS), ejection fraction (EF), and fractional shortening (FS) were calculated by the Pombo method using the system's software provided by the system.^{38,47} During the measurements, the vital signs of the rats were continuously monitored by a monitor (iPM8, Mindray, China).

CK-MB and LDH measurement

The collection of blood from the left ventricle of the heart occurred after a 6-hour observation of ROSC. The supernatant was obtained through centrifugation (4°C , 3500 g, 20 min). Myocardial tissue was examined by enzyme-linked immunosorbent assay. LDH activity and CK-MB were recorded.

Hematoxylin and eosin (H&E) staining

After the 6-hour post-ROSC experiment, we extracted heart tissue. Atrial sections were preserved at -80°C for analysis. Ventricular sections were fixed in 10% formalin, dehydrated in ethanol, paraffin-embedded, and 4 μm sections were prepared. Staining followed by microscopic examination of myocardial tissue sections was conducted at 40x10 magnification, ensuring a blinded and unbiased analysis.

Transmission electron microscopy (TEM)

TEM was the technique used to assess autophagosome variation in myocardial tissue. Ventricular tissues (1 mm^3) were initially fixed in 2.5% glutaraldehyde for 24 hours, followed by rinsing with PBS and subsequent fixation using 1% osmium tetroxide for 2 hours. After dehydration, staining, rehydration (using ethanol gradients of 30%, 50%, 70% acetate uranyl, 80%, 95%, and 100%), maceration, and embedding, 70 nm thick microtomes (Leica UC-7) were prepared. Finally, lead citrate staining was performed before examination with a JEM1400 electron microscope (Nippon Electron Corporation).

ATP measurement

Left ventricular tissue and H9c2 cells were harvested and lysed thoroughly by adding lysis buffer at a specified ratio. After lysis, samples underwent centrifugation at 12,000g for 5 minutes at 4°C , and the supernatant was collected. For ATP measurement, 100 μL of detection working solution was added to each well or tube, and the samples were allowed to equilibrate at room temperature for 3-5 minutes. Next, 20 μL of the lysed tissue and cell supernatant was added. ATP levels were measured using a luminometer (Beyotime S0027 Enhanced ATP Assay Kit).

ROS detection

We quantified intracellular ROS levels using the DCFH-DA Fluorescent Probe (Jiangsu Beyotime Biotechnology Co., Ltd.). DCFH-DA enters cells without fluorescence and is then converted to DCFH. The existence of ROS causes DCFH to oxidize, producing fluorescent DCF. The intensity of fluorescence is directly related to the concentration of ROS. After modeling and washing cardiomyocytes, we added a suitable dilution of DCFH-DA (serum-free medium: DCFH-DA=1000:1) and incubated it in the dark for 20 minutes. Finally, we measured DCF fluorescence intensity using flow cytometry (excitation: 488 nm, emission: 525 nm), which was analysed by FlowJo software.

MMP measurement

JC-1 dye assesses MMP, fluorescing red at high and green at low potentials by mixing JC-1 (200X), ultrapure water, and JC-1 staining buffer (5X) in a 1:160:40 proportion, a JC-1 staining solution was prepared. Cell culture medium and JC-1 stain were equal parts and the cells were

incubated for 20 minutes and then washed twice. MMP was measured by observing the red-to-green fluorescence ratio under an inverted microscope.

Western blotting

Myocardial tissue and H9c2 cell samples were prepared for Western blot analysis. We determined protein concentration using the BCA method. After separation of the proteins, the membrane was transferred, closed and incubated at low temperature with the following antibodies: phosphorylated Akt (Ser473, 1:2000, #4060, CST, USA), Akt (pan, 1:1000, #4691, CST, USA), phosphorylated-mTOR (Ser2448, 1:1000, #5536, CST, USA), mTOR (1:1000, #2983, CST, USA), LC3-II/I (1:2500, 14600-1-AP, proteintech, USA), Beclin 1 (1:2000, 66665-1-Ig, proteintech, USA), GAPDH(1:1000, ab181602, Abcam, UK), Goat Anti-Rabbit IgG (H+L) HRP(1:10000, Affinity, USA), and Goat Anti-Mouse IgG (H+L) HRP (1:10000, Affinity, USA). The following day, anti-rabbit IgG and anti-mouse IgG antibodies were co-incubated with the PVDF membrane for 2 hours at room temperature. Immunoblot band intensity was analyzed using Chemi-Smart 5100.

QUANTIFICATION AND STATISTICAL ANALYSIS

The statistical analysis of all experimental data was conducted using GraphPad Prism version 9.5.1, and FlowJo version 10.6.2. The Shapiro-Wilk test was employed to assess the normality of the data distribution. For comparisons between two datasets, the Mann-Whitney U test was utilized for data not following a normal distribution, while Student's t-test was applied for normally distributed data. In cases of multiple comparisons involving three or more groups, one-way ANOVA followed by Tukey's post hoc method was used. A two-sided p-value of less than 0.05 was considered statistically significant.